

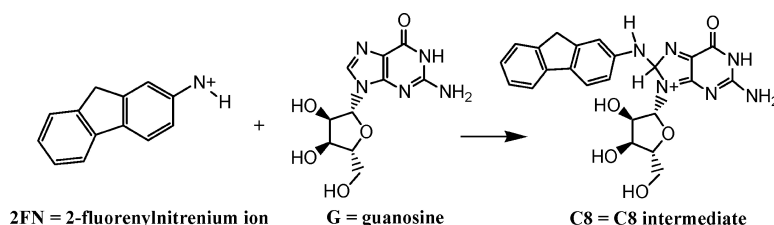
Communication

## Time-Resolved Resonance Raman Observation of the 2-Fluorenylnitrenium Ion Reaction with Guanosine to Form a C8 Intermediate

Pik Ying Chan, Wai Ming Kwok, Sze Kui Lam, Pauline Chiu, and David Lee Phillips

*J. Am. Chem. Soc.*, **2005**, 127 (23), 8246-8247 • DOI: 10.1021/ja0505651 • Publication Date (Web): 17 May 2005

Downloaded from <http://pubs.acs.org> on March 25, 2009



### More About This Article

Additional resources and features associated with this article are available within the HTML version:

- Supporting Information
- Links to the 8 articles that cite this article, as of the time of this article download
- Access to high resolution figures
- Links to articles and content related to this article
- Copyright permission to reproduce figures and/or text from this article

[View the Full Text HTML](#)



**ACS Publications**  
 High quality. High impact.

## Time-Resolved Resonance Raman Observation of the 2-Fluorenylnitrenium Ion Reaction with Guanosine to Form a C8 Intermediate

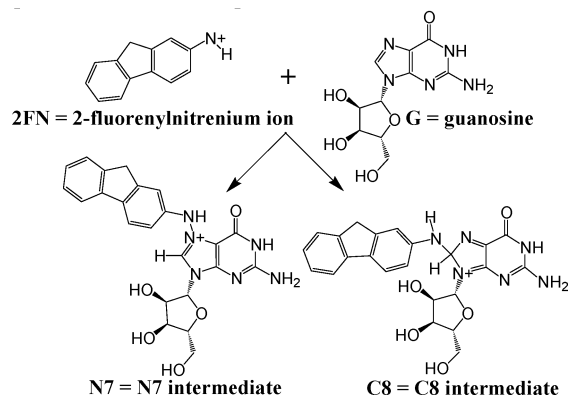
Pik Ying Chan, Wai Ming Kwok, Sze Kui Lam, Pauline Chiu, and David Lee Phillips\*

Department of Chemistry, The University of Hong Kong, Pokfulam Road, Hong Kong

Received January 28, 2005; E-mail: phillips@hkucc.hku.hk

There is much interest in the properties and chemical reactions of arylnitrenium ions since they likely play a key role in the chemical carcinogenesis of aromatic amines.<sup>1,2</sup> Aromatic amines, such as 2-acetylaminofluorene, can be enzymatically converted into the sulfate of the related *N*-hydroxylamines, and in aqueous environments, the sulfate spontaneously cleaves to produce an arylnitrenium ion.<sup>2a,d</sup> Arylnitrenium ions, such as the 2-fluorenylnitrenium ion (denoted as **2FN** hereafter), can be selectively trapped by guanine bases in DNA to cause damage<sup>1f,g,2b,3a</sup> that is thought to result in carcinogenic mutations. Arylnitrenium ions have been characterized by transient absorption (TA) spectroscopy,<sup>3,4</sup> time-resolved infrared (TRIR) spectroscopy,<sup>5</sup> and time-resolved resonance Raman (TR<sup>3</sup>) spectroscopy.<sup>6</sup> Using TA spectroscopy, McClelland and co-workers observed that the reaction of **2FN** with 2'-deoxyguanosine led to formation of a new intermediate tentatively assigned as an 8-(2-fluorenylamino)-2'-deoxyguanosine adduct or "C8 intermediate" based on several pieces of evidence.<sup>3</sup> There have been reports of evidence supporting arylnitrenium ions attacking guanine derivatives at the N7 position<sup>1f</sup> or at the C8 position (see Scheme 1).<sup>2c,3</sup>

**Scheme 1.** Proposed Reactions of the **2FN** with **G** to Form Either a C8 Intermediate or an N7 Intermediate



Herein, we report a TR<sup>3</sup> study of the reaction of **2FN** with guanosine (denoted **G** hereafter) to form a C8 intermediate species (denoted **C8** hereafter). To our knowledge, this is the first time-resolved vibrational spectroscopic characterization of an arylnitrenium ion reaction with a guanine derivative and of a C8 intermediate species. Figure 1A presents an overview of selected 369 nm TR<sup>3</sup> spectra obtained after 309 nm photolysis of 2-fluorenyl azide in the presence of **G** in an acetonitrile/water-buffered mixed solvent. The 10 ns spectrum is assigned to **2FN** that we have previously observed using TR<sup>3</sup> spectroscopy.<sup>6a,b,e</sup> The 10 ns spectrum in Figure 1A is very similar to and in good agreement with previous TR<sup>3</sup> spectra observed for **2FN** (see the Supporting Information for a comparison). The Raman bands due to **2FN** decrease on the hundreds of nanosecond time scale, and a new species appears to

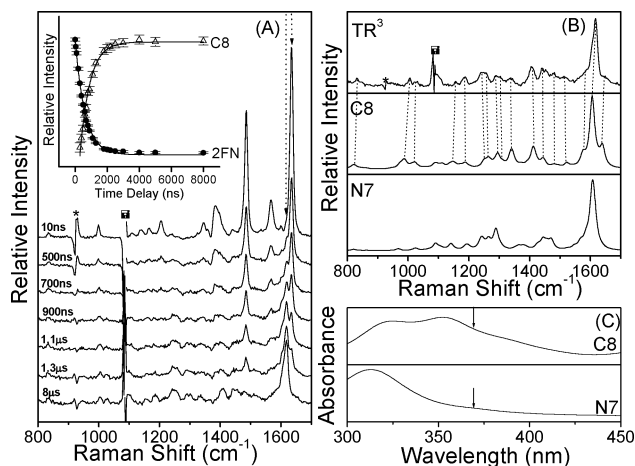


**Figure 1.** (A) Selected TR<sup>3</sup> spectra obtained after 309 nm photolysis of 2-fluorenyl azide in the presence of 1.8 mM **G** in a buffered 1:1 acetonitrile/water solution. The time delay between the probe and photolysis beams is given to the left of each spectrum. Plot of the integrated Raman band intensities of the decay and growth of the two marker bands (inset) indicated by the arrows as a function of time. The lines represent best fits of exponential decay and growth functions to the data. (B) Comparison of the 15 μs TR<sup>3</sup> spectrum to the BPW91/cc-PVDZ calculated Raman spectra for the **C8** and **N7** species. The dashed lines show the correspondence between the experimental TR<sup>3</sup> features and the predicted **C8** Raman bands. The asterisks indicate subtraction artifacts. (C) Computed absorption spectra for **C8** and **N7** (see text and Supporting Information for details).

be produced directly from it. The larger Raman bands in the 1600 cm<sup>-1</sup> region of the spectra (indicated by the arrows in Figure 1A) were used to follow the decay of **2FN** and the growth of the new species. Figure 1A (inset) presents a plot of the integrated intensities of the Raman marker bands indicated in Figure 1A. The decay of **2FN** and the growth of the new species were simultaneously fit satisfactorily by a common time constant ( $\tau \sim 615$  ns) exponential decay and growth functions, respectively, and this suggests the new species is directly produced from a reaction of **2FN**. This new species was only seen when **G** was present in the system and suggests that it is formed from the reaction of **2FN** with **G**. McClelland and Cheng<sup>3b</sup> used TA to study the same reaction of **2FN** with **G** and found that the reaction was first order in [**G**] and had a second-order rate constant of  $7.1 \times 10^8 \text{ M}^{-1} \text{ s}^{-1}$ . We found that the reaction monitored by TR<sup>3</sup> here was also first-order in [**G**] and gave a similar rate constant (see Supporting Information for details). BPW91/cc-PVDZ DFT calculations were found to predict the vibrational frequencies of both TRIR and TR<sup>3</sup> vibrational bands for a range of arylnitrenium ions,<sup>5,6</sup> and thus, they also are likely to work well for the related **C8** or **N7** species. BPW91/cc-PVDZ computations were done to calculate the optimized geometry and the corresponding Raman and absorption spectra for the lowest energy **C8** and **N7** formed from reaction of the **2FN** with **G**. In Figure 1B, the calculated Raman spectra are compared to the TR<sup>3</sup> spectrum of the new species observed at 15 μs. We note that

resonance enhancement of the TR<sup>3</sup> spectra may make the relative intensities of the Raman spectra different from those calculated for normal Raman spectra. When the chromophore for the enhancement is somewhat delocalized, the TR<sup>3</sup> and calculated normal Raman spectra can have similar intensity patterns, as was previously observed for the related 4-methoxyphenylnitrenium ion in ref 6d, and we expect that this is also the case here. Figure 1B reveals the Raman vibrational frequencies, and relative intensities calculated for **C8** agree well with the TR<sup>3</sup> spectrum of the second species while the **N7** calculated Raman spectrum does not agree very well. We tentatively assign the TR<sup>3</sup> spectrum of the reaction product to **C8** produced from reaction of the **2FN** and **G**. The calculated absorption spectra for **N7** and **C8** (Figure 1C) are noticeably different. The **C8** absorption has a strong band at 353 nm and substantial absorption at the 369 nm probe wavelength used in the TR<sup>3</sup> experiments, consistent with our assignment of **C8** to the second species in the TR<sup>3</sup> spectra. However, the **N7** absorption has a strong band at 316 nm and little absorption at 369 nm, and this suggests that our TR<sup>3</sup> experiment would not be very sensitive to **N7**.

In **C8** and **N7**, the most intense Raman bands are associated with the aromatic C=C stretches of the **FN** group near 1606 cm<sup>-1</sup>. The second most intense Raman bands in this region are the 1640 cm<sup>-1</sup> band associated the **G** moiety for **C8** and the 1614 cm<sup>-1</sup> band associated with the **FN** moiety of **N7**. This leads to the Raman spectra of **C8** and **N7** being distinctly different in this region, with the predicted **C8** Raman spectrum in good agreement with the experimental TR<sup>3</sup> spectrum while the predicted **N7** spectrum is not. The **C8** Raman spectrum also has substantial intensity in the 1338 cm<sup>-1</sup> (C-H bend) and 1411 cm<sup>-1</sup> (C-C stretch + C-H bend + O-H bend) Raman bands associated with the **G** moiety, and these bands are also in good agreement with the experimental TR<sup>3</sup> spectrum in Figure 1B. Similar features are very weak and not clearly discernible in the predicted **N7** Raman spectrum, and this does not agree with the experimental TR<sup>3</sup> spectrum. The fairly intense Raman bands at 1640, 1411, and 1338 cm<sup>-1</sup> associated with the **G** moiety serve to clearly distinguish **C8** and **N7**. This suggests the structures of the **G** moiety in these species are different from one another. The optimized geometry from the BPW91/cc-PVDZ calculations for **C8** and **N7** confirms this (see Figure S3 of the Supporting Information). In **C8**, the formation of the new C-N bond between **2FN** and **G** induces a large change in the bonding of ring 1 of **G**, so that the C<sup>25</sup>-N<sup>29</sup> (1.4989 Å) and C<sup>25</sup>-N<sup>26</sup> (1.4558 Å) bonds have single bond character, the N<sup>26</sup>-C<sup>27</sup> (1.3112 Å) and N<sup>29</sup>-C<sup>28</sup> (1.3406 Å) bonds have double bond character, and the C<sup>27</sup>-C<sup>28</sup> (1.4666 Å) bond has some single bond character. The attachment of **2FN** to the N7 position of **G** in **N7** results in a very different structure, where ring 1 of **G** retains the double bond character of the C<sup>25</sup>-N<sup>26</sup> bond, the single bond character of the N<sup>26</sup>-C<sup>27</sup> and N<sup>29</sup>-C<sup>28</sup> bonds, and the double bond character of the C<sup>27</sup>-C<sup>28</sup> bond, like that of a free **G** molecule. The formation of two C=N conjugated bonds in ring 1 of the **G** moiety of **C8** leads to significant Raman intensity in the 1640, 1411, and 1338 cm<sup>-1</sup> Raman bands of the **C8** Raman spectrum.

The first time-resolved vibrational spectroscopic observation of an aryl nitrenium ion reaction with a guanine derivative (**2FN** with **G**) and the formation of a **C8** intermediate species were reported. Comparison of the TR<sup>3</sup> spectra and previous TA spectra<sup>3b</sup> to predicted Raman and absorption spectra for **C8** and **N7** confirms that the reaction product observed from **2FN** with **G** is **C8**, in

agreement with the assignment proposed by McClelland and co-workers.<sup>3</sup> The Raman spectrum of **C8** exhibits significant intensity in modes associated with both the **FN** and **G** groups, and comparison with results from BPW91/cc-PVDZ computations indicates the **C8** species has two C=N conjugated bonds in ring 1 of the **G** moiety. We note our results do not rule out the possibility that an **N7** intermediate pathway may be in competition with the **C8** intermediate pathway, or that initial attack may be at **N7** and very quickly convert to the **C8** intermediate observed in the TR<sup>3</sup> spectra. Further work using different guanine derivatives should prove useful in better characterizing how **2FN** reacts with guanine derivatives. We also note the caveat that reactions with a free nucleoside in solution may be noticeably different than reactions that occur in guanine-containing oligomers or genomic DNA.

**Acknowledgment.** This work was supported by grants from the Research Grants Council of Hong Kong (HKU/7112/00P) to D.L.P. W.M.K. thanks The University of Hong Kong for the award of a Research Assistant Professorship.

**Supporting Information Available:** Description of the synthesis of the 2-fluorenyl azide precursor and TR<sup>3</sup> experiments. Figures of the TR<sup>3</sup> spectra and comparison to previous TR<sup>3</sup> spectra of **2FN**. Description of the BPW91/cc-PVDZ computations. Cartesian coordinates, total energies, and zero-point vibrational energies of the optimized geometry for the lowest energy **C8** and **N7** species. Simple schematic diagrams of **C8**, **N7**, **2FN**, and **G** with selected bond length parameters shown from BPW91/cc-PVDZ calculations. This material is available free of charge via the Internet at <http://pubs.acs.org>.

## References

- (1) (a) Miller, J. A. *Cancer Res.* **1970**, *20*, 559–576. (b) Miller, E. C. *Cancer Res.* **1978**, *38*, 1479–1496. (c) Miller, E. C.; Miller, J. A. *Cancer* **1981**, *47*, 2327–2345. (d) Garner, R. C.; Martin, C. N.; Clayson, D. B. In *Chemical Carcinogens*, 2nd ed.; Searle, C. E., Ed.; ACS Monograph 182: American Chemical Society: Washington, DC, 1984; Vol. 1, pp 175–276. (e) Famulok, M.; Boche, G. *Angew. Chem., Int. Ed. Engl.* **1989**, *28*, 468–469. (f) Humphreys, W. G.; Kadlubar, K. K.; Guengerich, F. P. *Proc. Natl. Acad. Sci. U.S.A.* **1992**, *89*, 8278–8282. (g) Kadlubar, F. F. In *DNA Adducts of Carcinogenic Amines*; Hemminki, K., Dipple, A., Shuker, D. E. G., Kadlubar, K. K., Segerbäch, D., Bartsch, H., Eds.; Oxford University Press: Oxford, U.K., 1994; pp 199–216. (h) Dipple, A. *Carcinogenesis* **1995**, *16*, 437–441.
- (2) (a) Novak, M.; Kahley, M. J.; Lin, J.; Kennedy, S. A.; James, T. G. *J. Org. Chem.* **1995**, *60*, 8294–8304. (b) Novak, M.; Kennedy, S. A. *J. Am. Chem. Soc.* **1995**, *117*, 574–575. (c) Kennedy, S. A.; Novak, M.; Kolb, B. A. *J. Am. Chem. Soc.* **1997**, *119*, 7654–7664. (d) Novak, M.; VandeWater, A. J.; Brown, A. J.; Sanzabacher, S. A.; Hunt, L. A.; Kolb, B. A.; Brooks, M. E. *J. Org. Chem.* **1999**, *64*, 6023–6031.
- (3) (a) McClelland, R. A.; Ahmad, A.; Dicks, A. P.; Licence, V. *J. Am. Chem. Soc.* **1999**, *121*, 3303–3310. (b) Cheng, B.; McClelland, R. A. *Can. J. Chem.* **2001**, *79*, 1881–1886.
- (4) (a) McClelland, R. A.; Davids, P. A.; Hadzialic, G. *J. Am. Chem. Soc.* **1995**, *117*, 4173–4174. (b) Srivastava, S.; Falvey, D. E. *J. Am. Chem. Soc.* **1995**, *117*, 10186–10193. (c) Michalak, J.; Zhai, H. B.; Platz, M. S. *J. Phys. Chem.* **1996**, *100*, 14028–14036. (d) McClelland, R. A.; Kahley, M. J.; Davids, P. A.; Hadzialic, G. *J. Am. Chem. Soc.* **1996**, *118*, 4794–4803. (e) Moran, R. J.; Falvey J. *Am. Chem. Soc.* **1996**, *118*, 8965–8966. (f) Chiapperino, D.; McLroy, S.; Falvey, D. E. *J. Am. Chem. Soc.* **2002**, *124*, 3567–3577. (g) Winter, A. H.; Falvey, D. E.; Cramer, C. J. *J. Am. Chem. Soc.* **2004**, *126*, 9661–9668.
- (5) (a) Srivastava, S.; Toscano, J. P.; Moran, R. J.; Falvey, D. E. *J. Am. Chem. Soc.* **1997**, *119*, 11552–11553. (b) Srivastava, S.; Ruane, P. H.; Toscano, J. P.; Sullivan, M. B.; Cramer, C. J.; Chiapperino, D.; Reed, E. C.; Falvey, D. E. *J. Am. Chem. Soc.* **2000**, *122*, 8271–8278.
- (6) (a) Zhu, P.; Ong, S. Y.; Chan, P. Y.; Leung, K. H.; Phillips, D. L. *J. Am. Chem. Soc.* **2001**, *123*, 2645–2649. (b) Zhu, P.; Ong, S. Y.; Chan, P. Y.; Poon, Y. F.; Leung, K. H.; Phillips, D. L. *Chem.—Eur. J.* **2001**, *7*, 4928–4936. (c) Chan, P. Y.; Ong, S. Y.; Zhu, P.; Leung, K. H.; Phillips, D. L. *J. Org. Chem.* **2003**, *68*, 5265–5273. (d) Chan, P. Y.; Ong, S. Y.; Zhu, P.; Zhao, C.; Phillips, D. L. *J. Phys. Chem. A* **2003**, *107*, 8067–8074. (e) Kwok, W. M.; Chan, P. Y.; Phillips, D. L. *J. Phys. Chem. B* **2004**, *108*, 19068–19075.

JA0505651